Magnetic structure of quasi-one-dimensional antiferromagnetic $TaFe_{1+y}Te_3$

X. Ke,[1,*] B. Qian,[2] H. Cao,[1] J. Hu,[2] G. C. Wang,[2] and Z. Q. Mao[2]

[1]*Quantum Condensed Matter Division, Oak Ridge National Laboratory, Oak Ridge, Tennessee 37831, USA*

[2]*Department of Physics and Engineering Physics, Tulane University, New Orleans, Louisiana 70118, USA*

(Received 14 January 2012; revised manuscript received 23 March 2012; published 6 June 2012)

We report the magnetic structure of $TaFe_{1+y}Te_3$ single crystals by means of neutron diffraction measurements. $TaFe_{1+y}Te_3$ possesses a layered structure with a formation of two-leg zigzag ladders along the b axis. We find that $TaFe_{1+y}Te_3$ undergoes an antiferromagnetic transition at 178 K with Fe1 spins of the intraladders ferromagnetically aligned and with Fe1 spins of the interladders antiferromagnetically coupled. Furthermore, spins of the neighboring interstitial Fe2 (y) ions align parallel to the Fe1 spins of each ladder. These findings are distinct from the magnetic structure of the recently discovered spin-ladder compound $BaFe_2Se_3$. $TaFe_{1+y}Te_3$ may serve as a model system for investigating the interesting physics of quasi-one-dimensional ferromagnetic systems.

DOI: 10.1103/PhysRevB.85.214404 PACS number(s): 75.25.−j, 74.70.Xa, 75.50.Ee

There has been intense interest in searching for new iron-based superconductors since the initial discovery of superconductivity in $La(O_{1-x}F_x)FeAs$ in 2008.[1] Many types of iron pnictide and iron chalcogenide superconductors have been discovered, including LnFeAs(O,F) (Ln = lanthanide) (1111),[2] $(A,K/Na)Fe_2As_2$ (A = Ba, Sr, Ca, Eu)[3] and $(Ba/Sr/Ca)(Fe,TM)_2As_2$ (TM = Co, Ni, Rh, Pd, Ir, Ru, Pt) (122),[4,5] $A_{1-x}FeAs$ (A = Li or Na) (111),[6] and Sr_2VO_3FeAs,[7] and $Fe_{1+y}(Te, Se)$ (11).[8] These materials share a common structural characteristic: Fe tetrahedrally coordinated by As or (Te, Se) to form square-planar sheets. The consensus is that magnetism and superconductivity are intimately correlated and compete with each other in these materials, as evidenced by the enhanced spin fluctuation above T_c,[9–17] the emergence of spin resonance,[11,13–15] and the suppression of magnetism below T_c.[18] Studies of the magnetic structure and spin dynamics of these materials have played a key role in understanding mechanisms of superconductivity and exploring for new superconductors.

In addition to 1111-, 122-, 111- and 11-type materials, several other types of Fe-based materials have recently been investigated, including $A_2Fe_4Se_5$,[19–23] with A = Rb, Cs, (Tl, Rb/K); $BaFe_2Se_3$;[24–26] and $TaFe_{1+y}Te_3$.[27] Some of these materials are found to be superconducting,[19–23] while some are not.[25–27] $TaFe_{1+y}Te_3$, the material studied in this paper, was discovered[28] about two decades ago and was recently revisited by Liu *et al.*[27] This compound possesses a $P2_1/m$ monoclinic crystal structure, with the lattice parameters a = 7.436 Å, b = 3.638 Å, c = 10.008 Å, and β = 109.17°.[28] The Ta-Fe bonded network lies between Te layers, forming a $FeTaTe_3$ "sandwich,"[27,28] as shown in Fig. 1(a). The excess Fe (y) ions partially occupy a square pyramidal site. Similar to $BaFe_2Se_3$,[24–26] Fe ions form two-leg ladders along a principle axis (b axis) in $TaFe_{1+y}Te_3$ but with a zigzag shape instead of rectangular one, thus representing another intriguing quasi-one-dimensional magnetic system. $TaFe_{1.25}Te_3$ (y = 0.25) has a structural phase transition at 1010 K, and orders antiferromagnetically below 200 K.[28] Interestingly, this material displays metallic behavior down to 4 K.[27,28] Detailed susceptibility, magnetoresistance, and Hall effect measurements[27] suggest that the antiferromagnetic (AFM) transition is of a spin-density-wave character and that the Fe1 moment is ∼3.7 μ_B/Fe and the Fe2 (i.e., interstitial Fe ion) moment is ∼4 μ_B/Fe. Furthermore, it was proposed that neighboring spins within each zigzag ladder aligned antiferromagnetically while spins between neighboring ladders are ferromagnetically coupled.[27] However, this needs to be validated by other techniques, such as neutron scattering studies, which were not available until this work.

In this paper, we report the magnetic structure of $TaFe_{1+y}Te_3$ (y = 0.17) revealed by single-crystal neutron diffraction measurements. In sharp contrast to what has been proposed by Liu *et al.*,[27] we found that in the AFM state of $TaFe_{1+y}Te_3$, the Fe spins within each ladder are aligned parallel to each other in the $[1\,0\,-1]_r$ direction in real space while spins between ladders are antiferromagnetically coupled. Furthermore, the magnetic moment of interstitial Fe2, which is randomly sited, prefers to be parallel to the Fe1 spins of each ladder, as illustrated in Fig. 1(b). This suggests a strong ferromagnetic exchange interaction of Fe1 spins along the zigzag rungs (J_{nn}), rendering the system a quasi-one-dimensional ferromagnet. Such a peculiar magnetic structure is dramatically different from that of $BaFe_2Se_3$, with a crystal structure also composed of two-leg ladders.

Single crystals of $TaFe_{1+y}Te_3$ were grown using a chemical vapor transport method, as described in earlier literature.[27,28] Powders of the raw materials Ta, Fe, and Te with a nominal molar ratio of 1:1.25:3 were ground and then sealed in an evacuated quartz tube, together with $TeCl_4$ that serves as a transporting agent. The tube was then placed in a furnace and slowly heated, with the hot end at 690 °C and the cool end at 660 °C. The furnace was cooled to room temperature after 1 week of growth time. The typical dimensions of single crystals grown with this method are ∼3 × 4 × 0.5 mm^3. The structure of the crystals was characterized by x-ray diffraction. The electronic and magnetic properties of crystals were measured using a Quantum Design physical property measurement system and superconducting quantum interference device magnetometer, respectively. To obtain the magnetic structure of this material, a single crystal with a mass of ∼11 mg was measured using the four-circle neutron diffractometer HB-3A located at the High Flux Isotope Reactor, Oak Ridge National

 ©2012 American Physical Society

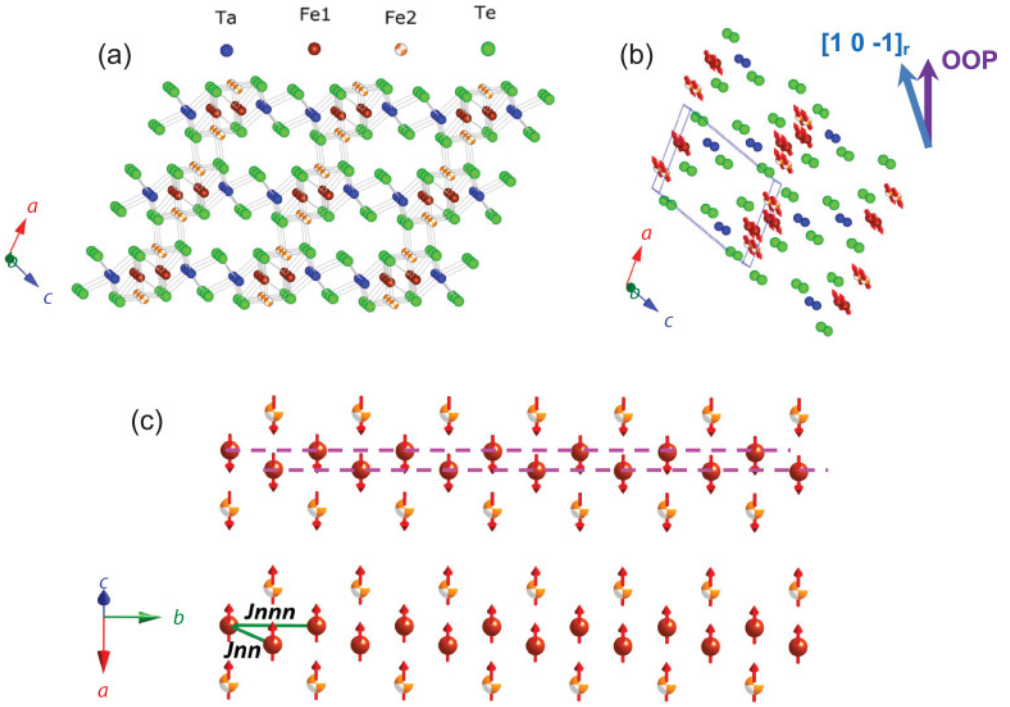

FIG. 1. (Color online) Schematics of the (a) monoclinic crystal structure and (b) spin structure, and (c) detailed view of the zigzag ladders of $TaFe_{1+y}Te_3$. Fe1 sites are fully occupied, while Fe2 sites represented by a different symbol are only partially occupied. The inset in (b) shows the OOP direction, $[1\,0\,-1]_{rec}$ in reciprocal space, which is perpendicular to the cleaved plane and tilts from the $[1\,0\,-1]_r$ direction in real space (i.e., the moment direction) by 17.6°. The pink dashed lines in (c) illustrate two nearest-neighboring Fe1 chains forming a zigzag ladder.

Laboratory. A neutron wavelength of 1.536 Å[29] was used, unless noted otherwise, by using a double-focusing Si(2 2 0) monochromator.

Figure 2(a) shows the temperature dependence of magnetization of $TaFe_{1+y}Te_3$ measured with a magnetic field of 1000 Oe applied along in-plane (IP) and out-of-plane (OOP) directions. The OOP direction, $[1\,0\,-1]_{rec}$ in reciprocal space, represents the direction that is perpendicular to the layer plane of the sample (i.e., the cleaved surface of the sample), and it has ∼17.6° tilt from the $[1\,0\,-1]_r$ direction in real space, which is the direction of the magnetic moments, as shown in Fig. 1. The magnetization shows a maximum ∼178 K, and field-cooled and zero field-cooled measurements do not show any noticeable difference, which indicates the onset of an AFM transition. As noted earlier, the previously reported AFM transition temperature T_N for a $TaFe_{1.25}Te_3$ powder sample is ∼200 K, ∼20 K higher than the transition temperature observed in our sample; this discrepancy may be due to the lower Fe2 concentration ($y < 0.25$) in our sample, as confirmed by the neutron diffraction measurements shown later. The larger suppression of magnetization with the field along the OOP direction than that along the IP direction suggests the nature of magnetic anisotropy with the spin easy axis tilt towards the OOP direction.

In Fig. 2(b), we plot the resistivity as a function of temperature measured with a direct current ($I = 1$ mA) applied along the IP and OOP directions. The data were taken using a standard four-probe method. For the current applied along the IP direction, the material exhibits metallic behavior over the whole measured temperature range. In addition, the

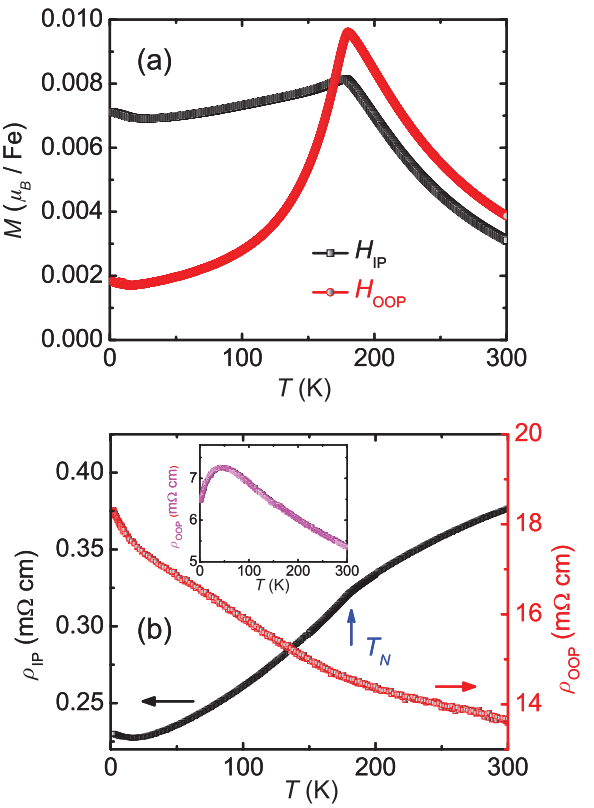

FIG. 2. (Color online) Temperature dependence of (a) magnetization and (b) resistivity of $TaFe_{1+y}Te_3$ along both IP and OOP directions. The exact IP directions measured are not specified.

AFM transition results in a steeper decrease in resistivity and a kink near T_N. These characteristics are indicative of an itinerant antiferromagnet. However, the resistivity along the OOP direction of most samples we measured exhibits nonmetallic behavior in the whole temperature range [main panel of Fig. 2(b)], with $\rho_{OOP}/\rho_{IP} \approx 50$ at $T = 2$ K. Such an anisotropic behavior in electronic transport is associated with the layered crystal structure and magnetic structure, as discussed later. Occasionally, a metallic feature is observed at low temperature along the OOP direction, as shown in the inset of Fig. 1(b), which may originate from rich excess Fe that helps interplane bonding and enhances conductivity.

To characterize the nuclear and magnetic structure of $TaFe_{1+y}Te_3$, we performed single-crystal neutron diffraction measurements at various temperatures between 5 K and room temperature. The crystal structure refined from the neutron scattering data collected at 5 K [Fig. 1(a)] does not show any essential difference from the room temperature structure except for a slight thermal contraction of the lattice. Data refinement using Fullprof[30] with the refinement shown in Fig. 4(a) reveals a smaller concentration of interstitial Fe ions than the expected nominal value, with $y = 0.172$ (8), which may explain the lower T_N value in our single-crystal sample compared to the previously reported value (~200 K) for $TaFe_{1.25}Te_3$.[28] Furthermore, no superlattice peaks are observed, indicative of the random occupancy of Fe2 interstitials; this is consistent with the previous x-ray and transmission electron microscopy results.[28]

In addition to the nuclear Bragg diffraction, neutron scattering intensities show peaks in (H K L), with half-integer values of H and L. For instance, Fig. 3(a) plots the rocking curve measurements of (0.5 0 0.5) and (− 0.5 0 0.5) magnetic Bragg peaks taken at $T = 5$ K using a neutron wavelength of 2.410 Å that does not have the half-λ contamination, which shows a nice Gaussian shape with the full width at half maximum defined by the instrumental resolution. The magnetic form factor associated with the magnitude of (0.5 0 0.5) and (−0.5 0 0.5) **Q** vectors is almost the same; thus, the difference in the diffraction intensity of these two **Q** vectors originates from their relative direction to the magnetic moment. Such diffractions with half-integer values of H and L are ascribed to the AFM diffractions. This is clearly evidenced by the temperature dependence of (0.5 0 0.5) magnetic diffraction intensity shown in Fig. 3(b), and the gradual increase in intensity below $T_N \approx 178$ K is characteristic of a second-order phase transition, in agreement with both transport and magnetic susceptibility measurements presented in Fig. 2.

We measured a series of magnetic diffraction peaks at $T = 5$ K to determine and refine the magnetic structure of $TaFe_{1+y}Te_3$. The magnetic ordering propagation vector is determined to be (−0.5 0 0.5) in reciprocal space, and there are four irreducible representations for both Fe1 and Fe2 to describe the magnetic structure using the BasIresps program in Fullprof.[30] These include parallel/antiparallel spin alignment along the b axis or in the ac plane. We refined the magnetic diffraction data (including 40 magnetic reflections) in terms of 16 possible magnetic structures (combining both Fe1 and Fe) and found that the magnetic structure shown in Fig. 1(b) yields the best fit to the data with $R_F = 0.088$ and $\chi^2 = 1.425$, as manifested in the consistency of calculated and measured

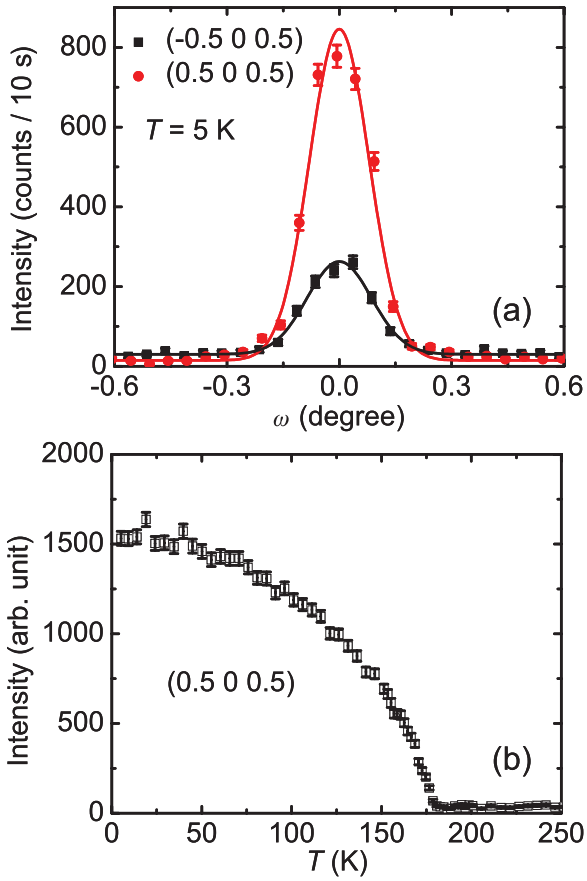

FIG. 3. (Color online) (a) Rocking curve of magnetic reflections (− 0.5 0 0.5) and (0.5 0 0.5) at $T = 5$ K. (b) Temperature dependence of (0.5 0 0.5) magnetic peak intensity. Solid curves are Gaussian fits.

intensity displayed in Fig. 4(b), while refinements with other types of magnetic structure give a χ^2 value at least larger than 7.820. This magnetic structure possesses the following remarkable characteristics: (1) Fe1 spins along the chain direction (b axis) are parallel; (2) Fe1 spins of two neighboring chains also point in a parallel direction, thus forming a ferromagnetic two-leg zigzag ladder; (3) the spin direction of neighboring interstitial Fe2 of each ladder prefers to align parallel to the Fe1 spin direction; and (4) spins of neighboring zigzag ladders align antiparallel to each other in the ac plane. A closer look of the Fe spin configuration is in Fig. 1(c). The magnetic moment points along the $[1\,0\,-1]_r$ direction in real space, consistent with the magnetic susceptibility results plotted in Fig. 2(a) that shows a larger magnetic susceptibility value along the OOP direction. In addition, the moment size extracted from data refinement is 2.1 (1) μ_B/Fe for Fe1 and 2.6 (1) μ_B/Fe for Fe2, both of which are smaller than the expected values for the high spin states of Fe^{2+} ($3d^4$) and Fe^{3+} ($3d^5$). The valence values of Fe1 and Fe2 may be a mixture of both Fe^{2+} and Fe^{3+}. The suppression of magnetic moment is presumably associated with the itinerancy of charge carriers, as evidenced by the metallic electronic transport feature shown in Fig. 2(b).

Such a magnetic structure of $TaFe_{1+y}Te_3$ is in sharp contrast to the one proposed recently by Liu *et al.*[27] that is composed of AFM zigzag chains of Fe1 with the neighboring ladders

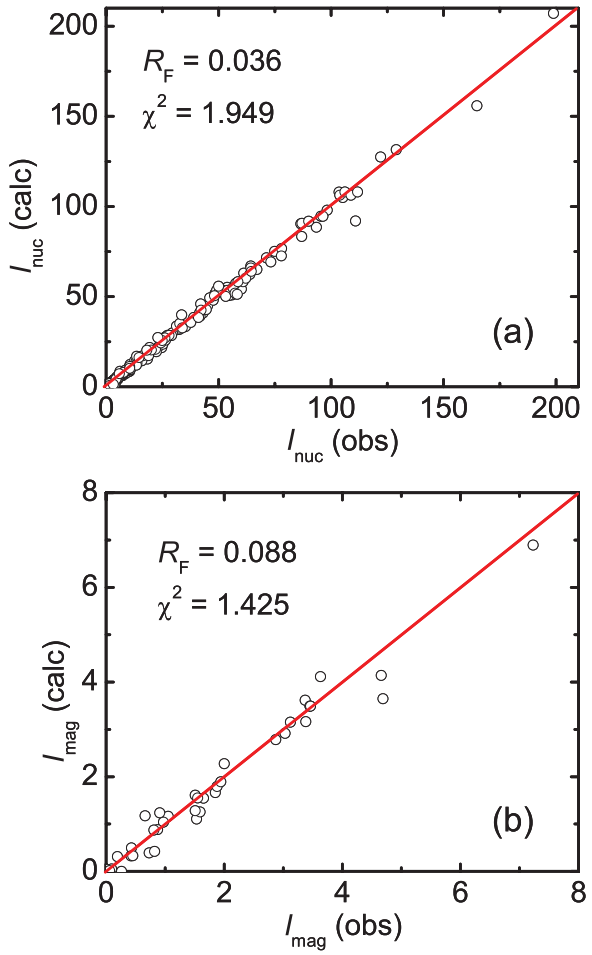

FIG. 4. (Color online) Plots of the comparison of observed and calculated intensities of various (a) nuclear and (b) magnetic diffraction peaks, showing the quality of data refinement. Red lines are visual guides.

couple ferromagnetically below T_N. Data refinement using the magnetic structure proposed by Liu *et al.* results in a poor fit, with $R_F = 0.74$ and $\chi^2 = 210$, suggesting this type of magnetic structure is not the right one. This magnetic structure is also distinct from the antiferromagnetically coupled checkerboards consisting of four ferromagnetically aligned spins observed in $BaFe_2Se_3$,[25] which is also a quasi-one-dimensional system but with an orthorhombic crystal structure. Our newly obtained spin structure suggests that the magnetic coupling of the nearest-neighboring Fe1 spins of the zigzag ladders in $TaFe_{1+y}Te_3$, J_{nn} shown in Fig. 1(c), are ferromagnetic, which may be dominated by the direct exchange interaction between Fe1 spins considering the short Fe1-Fe1 distance (2.72 Å) that is slightly longer than the interatomic distance of Fe metal (~2.53 Å). In addition, the exchange interaction with the next nearest-neighboring Fe1 spin along the chain direction, J_{nnn}, may be ferromagnetic, mainly due to the almost 90°-exchange path of Fe1-Te-Fe1. We speculate that the parallel spin alignment of Fe2 to Fe1 may originate from the ferromagnetic direct exchange interaction because of the short distance (~2.49 Å). These ferromagnetic exchange interactions lead to the parallel spin alignment of each zigzag ladder and the Fe2 interstitials, which consequently inhibits the occurrence of superconductivity at low temperatures. Detailed first-principles calculations and inelastic neutron scattering measurements are warranted to clarify the nature of these magnetic interactions.

Now let's turn to the magnetic coupling between neighboring ladders. The antiparallel spin alignment between neighboring ladders indicates an AFM interaction that induces the observed paramagnetic–AFM transition below $T_N \approx 178$ K. As shown in Fig. 1(a), however, we speculate that the superexchange interaction between Fe1 ions of neighboring ladders along both the OOP direction (interlayer) and the IP direction is relatively weak and much smaller than the energy scale of the transition temperature, considering that the shortest distance of these Fe1 ions in ~6.78 and 8.54 Å, respectively. Thus, $TaFe_{1+y}Te_3$ can be regarded as a quasi-one-dimensional ferromagnetic system. This appears to be a one-dimensional analog of the quasi-two-dimensional ferromagnetic $Ca_3Ru_2O_7$,[31,32] where ferromagnetically coupled bilayers are stacked antiferromagnetically along the OOP direction. A possible mechanism that drives the AFM transition in $TaFe_{1+y}Te_3$ is via the superexchange interaction involving Fe2 interstitials, which requires further investigations.

While $TaFe_{1+y}Te_3$ is not superconducting, which might be associated with its ferromagnetic zigzag ladder structure, as described previously, the magnetism of this quasi-one-dimensional material is quite intriguing. Low-dimensional magnetism, particularly in one-dimensional systems, has been the subject of intense research interest in the past decades. Even though most materials studied so far have AFM exchange interaction along the chain direction, materials with ferromagnetic spin chains, such as $LaCrOS_2$,[33] $CaVO_3$,[34] $CsNiF_3$,[35] $CoNb_2O_6$,[36] and some organic materials,[37,38] have also been found to have interesting physics. The examples include magnetic soliton-like behavior found in $CsNiF_3$[35] and the recently discovered continuous quantum phase transition tuned by external magnetic fields in $CoNb_2O_6$.[36] Since $TaFe_{1+y}Te_3$ possesses the peculiar quasi-one-dimensional ferromagnetic spin structure, as discussed previously, further investigations may prove that it serves as a model system for exploring novel physics of low-dimensional ferromagnetism.

In summary, we have investigated electronic and magnetic properties of $TaFe_{1+y}Te_3$ single crystals through resistivity, magnetization, and neutron scattering measurements. The magnetic structure of this compound has been determined from the refinement of neutron diffraction data. We found that its magnetic ordered state is composed of ferromagnetic two-leg zigzag ladders that are antiferromagnetically coupled to their neighbors along both IP and OOP directions, distinct from the magnetic structure conjectured based on magnetotransport measurements reported in Ref. 27.

Research at Oak Ridge National Laboratory's High Flux Isotope Reactor was sponsored by the Scientific User Facilities Division, Office of Basic Energy Sciences, US Department of Energy. Work at Tulane University is supported by the US National Science Foundation under Grant No. DMR-1205469 and the Louisiana Alliance for Simulation-Guided Materials Applications program under Award No. EPS-1003897. X.K. gratefully acknowledges the financial support by the Clifford G. Shull Fellowship at Oak Ridge National Laboratory.

*kex1@ornl.gov

[1] Y. Kamihara, T. Watanabe, M. Hirano, and H. Hosono, J. Am. Chem. Soc. **130**, 3296 (2008).

[2] X. H. Chen, T. Wu, G. Wu, R. H. Liu, H. Chen, and D. F. Fang, Nature **453**, 761 (2008); G. F. Chen, Z. Li, D. Wu, G. Li, W. Z. Hu, J. Dong, P. Zheng, J. L. Luo, and N. L. Wang, Phys. Rev. Lett. **100**, 247002 (2008); Z.-A. Ren, W. Lu, J. Yang, W. Yi, X.-L. Shen, Z.-C. Li, G.-C. Che, X.-L. Dong, L.-L. Sun, F. Zhou, and Z.-X. Zhao, Chin. Phys. Lett. **25**, 2215 (2008); H.-H. Wen, G. Mu, L. Fang, H. Yang, and X. Zhu, Europhys. Lett. **82**, 17009 (2008).

[3] M. Rotter, M. Tegel, and D. Johrendt, Phys. Rev. Lett. **101**, 107006 (2008); G.-F. Chen, Z. Li, G. Li, W.-Z. Hu, J. Dong, J. Zhou, X.-D. Zhang, P. Zheng, N.-L. Wang, and J.-L. Luo, Chin. Phys. Lett. **25**, 3403 (2008); K. Sasmal, B. Lv, B. Lorenz, A. M. Guloy, F. Chen, Y.-Y. Xue, and C.-W. Chu, Phys. Rev. Lett. **101**, 107007 (2008); M. S. Torikachvili, S. L. Bud'ko, N. Ni, and P. C. Canfield, *ibid.* **101**, 057006 (2008); H. S. Jeevan, Z. Hossain, D. Kasinathan, H. Rosner, C. Geibel, and P. Gegenwart, Phys. Rev. B **78**, 092406 (2008).

[4] A. S. Sefat, R. Jin, M. A. McGuire, B. C. Sales, D. J. Singh, and D. Mandrus, Phys. Rev. Lett. **101**, 117004 (2008).

[5] See a review, P. C. Canfield and S. L. Bud'ko, Annu. Rev. Matter. Phys. **1**, 27 (2010), and references therein.

[6] X. C. Wang, Q. Q. Liu, Y. X. Lv, W. B. Gao, L. X. Yang, R. C. Yu, F. Y. Li, and C. Q. Jin, Solid State Comm. **148**, 538 (2008); M. J. Pitcher, D. R. Parker, P. Adamson, S. J. C. Herkelrath, A. T. Boothroyd, R. M. Ibberson, M. Brunelli, and S. J. Clarke, Chem. Commun. 5918 (2008); J. H. Tapp, Z. Tang, B. Lv, K. Sasmal, B. Lorenz, P. C. W. Chu, and A. M. Guloy, Phys. Rev. B **78**, 060505 (2008).

[7] X. Zhu, F. Han, G. Mu, P. Cheng, B. Shen, B. Zeng, and H.-H. Wen, Phys. Rev. B **79**, 220512 (2009).

[8] F. C. Hsu, J. Y. Luo, K. W. Yeh, T. K. Chen, T. W. Huang, P. M. Wu, Y. C. Lee, Y. L. Huang, Y. Y. Chu, D. C. Yan, and M. K. Wu, Proc. Natl. Acad. Sci. USA **105**, 14262 (2008); M. H. Fang, H. M. Pham, B. Qian, T. J. Liu, E. K. Vehstedt, Y. Liu, L. Spinu, and Z. Q. Mao, Phys. Rev. B **78**, 224503 (2008).

[9] K. Ahilan, F. L. Ning, T. Imai, A. S. Sefat, R. Jin, M. A. McGuire, B. C. Sales, and D. Mandrus, Phys. Rev. B **78**, 100501 (2008).

[10] Y. Nakai, K. Ishida, Y. Kamihara, M. Hirano, and H. Hosono, J. Phys. Soc. Jpn. **77**, 073701 (2008).

[11] A. D. Christianson, E. A. Goremychkin, R. Osborn, S. Rosenkranz, M. D. Lumsden, C. D. Malliakas, I. S. Todorov, H. Claus, D. Y. Chung, M. G. Kanatzidis, R. I. Bewley, and T. Guidi, Nature **456**, 930 (2008).

[12] T. Imai, K. Ahilan, F. L. Ning, T. M. McQueen, and R. J. Cava, Phys. Rev. Lett. **102**, 177005 (2009).

[13] M. D. Lumsden, A. D. Christianson, D. Parshall, M. B. Stone, S. E. Nagler, G. J. MacDougall, H. A. Mook, K. Lokshin, T. Egami, D. L. Abernathy, E. A. Goremychkin, R. Osborn, M. A. McGuire, A. S. Sefat, R. Jin, B. C. Sales, and D. Mandrus, Phys. Rev. Lett. **102**, 107005 (2009).

[14] S. Chi, A. Schneidewind, J. Zhao, L. W. Harriger, L. Li, Y. Luo, G. Cao, Z. Xu, M. Loewenhaupt, J. Hu, and P. Dai, Phys. Rev. Lett. **102**, 107006 (2009); S. Li, Y. Chen, S. Chang, J. W. Lynn, L. Li, Y. Luo, G. Cao, Z. Xu, and P. Dai, Phys. Rev. B **79**, 174527 (2009).

[15] Y. Qiu, W. Bao, Y. Zhao, C. Broholm, V. Stanev, Z. Tesanovic, Y. C. Gasparovic, S. Chang, J. Hu, B. Qian, M. Fang, and Z. Mao, Phys. Rev. Lett. **103**, 067008 (2009).

[16] M. D. Lumsden, A. D. Christianson, E. A. Goremychkin, S. E. Nagler, H. A. Mook, M. B. Stone, D. L. Abernathy, T. Guidi, G. J. MacDougall, C. dela Cruz, A. S. Sefat, M. A. McGuire, B. C. Sales, and D. Mandrus, Nat. Phys. **6**, 182 (2010).

[17] H. A. Mook, M. D. Lumsden, A. D. Christianson, S. E. Nagler, B. C. Sales, R. Jin, M. A. McGuire, A. S. Sefat, D. Mandrus, T. Egami, and C. dela Cruz, Phys. Rev. Lett. **104**, 187002 (2010).

[18] S. Nandi, M. G. Kim, A. Kreyssig, R. M. Fernandes, D. K. Pratt, A. Thaler, N. Ni, S. L. Bud'ko, P. C. Canfield, J. Schmalian, R. J. McQueeney, and A. I. Goldman, Phys. Rev. Lett. **104**, 057006 (2010); D. K. Pratt, W. Tian, A. Kreyssig, J. L. Zarestky, S. Nandi, N. Ni, S. L. Bud'ko, P. C. Canfield, A. I. Goldman, and R. J. McQueeney, *ibid.* **103**, 087001 (2009).

[19] J. Guo, S. Jin, G. Wang, S. Wang, K. Zhu, T. Zhou, M. He, and X. Chen, Phys. Rev. B **82**, 180520(R) (2010).

[20] A. F. Wang, J. J. Ying, Y. J. Yan, R. H. Liu, X. G. Luo, Z. Y. Li, X. F. Wang, M. Zhang, G. J. Ye, P. Cheng, Z. J. Xiang, and X. H. Chen, Phys. Rev. B **83**, 060512(R) (2011).

[21] W. Bao, Q. Huang, G. F. Chen, M. A. Green, D. M. Wang, J. B. He, X. Q. Wang, and Y. Qiu, Chin. Phys. Lett. **28**, 086104 (2011).

[22] F. Ye, S. Chi, W. Bao, X. F. Wang, J. J. Ying, X. H. Chen, H. D. Wang, C. H. Dong, and M. Fang, Phys. Rev. Lett. **107**, 137003 (2011).

[23] B. C. Sales, M. A. McGuire, A. F. May, H. Cao, B. C. Chakoumakos, and A. S. Sefat, Phys. Rev. B **83**, 224510 (2011).

[24] A. Krzton-Maziopa, E. Pomjakushina, V. Pomjakushin, D. Sheptyakov, D. Chernyshov, V. Svitlyk, and K. Conder, J. Phys. Condens. Matter **23**, 402201 (2011).

[25] J. M. Caron, J. R. Neilson, D. C. Miller, A. Llobet, and T. M. McQueen, Phys. Rev. B **84**, 180409(R) (2011).

[26] B. Saparov, S. Calder, B. Sipos, H. Cao, S. Chi, D. J. Singh, A. D. Christianson, M. D. Lumsden, and A. S. Sefat, Phys. Rev. B **84**, 245132 (2011).

[27] R. H. Liu, M. Zhang, P. Cheng, Y. J. Yan, Z. J. Xiang, J. J. Ying, X. F. Wang, A. F. Wang, G. J. Ye, X. G. Luo, and X. H. Chen, Phys. Rev. B **84**, 184432 (2011).

[28] M. E. Badding, J. Li, F. J. Disalvo, W. Zhou, and P. P. Edwards, J. Solid State Chem. **100**, 313 (1992).

[29] B. C. Chakoumakos, H. Cao, F. Ye, A. D. Stoica, M. Poovici, M. Sundaram, W. Zhou, J. S. Kicks, G. W. Lynn, and R. A. Riedel, J. Appl. Crystallogr. **44**, 655 (2011).

[30] J. Rodriguez-Carvajal, Phys. B **192**, 55 (1993).

[31] W. Bao, Z. Q. Mao, Z. Qu, and J. W. Lynn, Phys. Rev. Lett. **100**, 247203 (2008).

[32] X. Ke, T. Hong, J. Peng, S. E. Nagler, G. E. Granroth, M. D. Lumsden, and Z. Q. Mao, Phys. Rev. B **84**, 014422 (2011).

[33] Y. Takano, T. Tsubaki, C. Itoi, K. Takase, K. Sekizawa, Solid State Comm. **122**, 661 (2002).

[34] A. A. Tsirlin, O. Janson, and H. Rosner, Phys. Rev. B **84**, 144429 (2011).

[35] J. K. Kjems and M. Steiner, Phys. Rev. Lett. **41**, 1137 (1978).

[36] R. Coldea, D. A. Tennant, E. M. Wheeler, E. Wawrzynska, D. Prabhakaran, M. Telling, K. Habicht, P. Smeibidl, and K. Kiefer, Science **327**, 177 (2010).

[37] C. P. Landee and R. D. Willett, Phys. Rev. Lett. **43**, 463 (1979).

[38] T. Sugano, S. J. Blundell, T. Lancaster, F. L. Pratt, and H. Mori, Phys. Rev. B **82**, 180401(R) (2010).